

# **Co-doped $\text{La}_{1-x}\text{Sr}_x\text{TiO}_{3-\delta}$ : A Diluted Magnetic Oxide System with High Curie Temperature**

Y. G. Zhao<sup>1,¶</sup>, S. R. Shinde<sup>1</sup>, S. B. Ogale<sup>1,\*</sup>, J. Higgins<sup>1</sup>, S. E. Lofland<sup>2</sup>, C. Lanci<sup>2</sup>, J. P. Buban<sup>3</sup>, N. D. Browning<sup>3</sup>, S. Das Sarma<sup>4</sup>, A. J. Millis<sup>5</sup>, V.N. Kulkarni<sup>1,§</sup>, R. J. Choudhary<sup>1</sup>, R. L. Greene<sup>1</sup>, T. Venkatesan<sup>1</sup>.

<sup>1</sup>Center for Superconductivity Research, Department of Physics, University of Maryland, College Park, MD 20742-4111.

<sup>2</sup>Department of Chemistry and Physics, Rowan University, Glassboro, N.J. 08028-1701.

<sup>3</sup>Department of Physics, University of Illinois at Chicago, 845 West Taylor Street, Chicago, IL 60607-7059.

<sup>4</sup>Condensed Matter Theory Center, Department of Physics, University of Maryland, College Park, MD 20742-4111.

<sup>5</sup>Department of Physics, Columbia University, 538 West 120<sup>th</sup> Street, New York, New York 10027.

## Abstract

Ferromagnetism is observed at and above room temperature in pulsed laser deposited epitaxial films of Co-doped Ti-based oxide perovskite ( $\text{La}_{1-x}\text{Sr}_x\text{TiO}_{3-\delta}$ ). The system has the characteristics of an intrinsic diluted magnetic semiconductor (metal) at low concentrations ( $< \sim 2\%$ ), but develops inhomogeneity at higher cobalt concentrations. The films range from being opaque metallic to transparent semiconducting depending on the oxygen pressure during growth and are yet ferromagnetic.

Induction of ferromagnetism in non-magnetic host materials by doping of magnetic impurities in dilute concentrations has gained considerable attention recently because of the addition of spin functionality to the original property-set of the concerned host [1]. This strategy for new materials development is of key significance to the emerging field of spintronics [1,2]. During the past few years considerable success has been achieved in the synthesis of diluted magnetic semiconductors (DMS) based on III-V semiconductors [3]. More recently room temperature ferromagnetism has also been reported in some magnetic impurity doped oxide based systems [4-7]. In this context the report of room temperature ferromagnetism in Co doped anatase  $\text{TiO}_2$  by Matsumoto et al. [7] is particularly interesting, opening an avenue for exploration of ferromagnetism in other titanium oxide systems. Unfortunately, attempts to induce ferromagnetism in Ti-based oxides such as  $\text{LaTiO}_3$  and  $\text{SrTiO}_3$  have not met with success [8], possibly due to the rather small number of carriers in these systems. Indeed it has been shown that the ferromagnetism in DMS depends strongly and non-trivially on the carrier density and the concentration of the magnetic ions [9], as well as on the magnetic coupling between the carriers and the magnetic ions.

Here we examine the case of cobalt doping in the mixed state of the end compounds  $\text{LaTiO}_3$  and  $\text{SrTiO}_3$ , namely the Ti-based perovskite  $\text{La}_{1-x}\text{Sr}_x\text{TiO}_3$  (LSTO), and show that ferromagnetism at and above room temperature can indeed occur in this system. It is suggested that the mixed-valent strongly correlated character of the compound provides favorable ground for ferromagnetic coupling between the magnetic ions [10]. Indeed the electrical transport properties of this material can be tuned dramatically with  $x$ , changing it from an insulator to a metal [11].  $\text{LaTiO}_3$  ( $x=0$ ), shows

nonmetallic behavior due to strong correlation [12], which also leads to antiferromagnetic ordering [12,13]. With slight La/O off-stoichiometry or Sr doping, the antiferromagnetic ordering disappears and an insulator-metal transition occurs [12-14]. The carrier density of  $\text{La}_{1-x}\text{Sr}_x\text{TiO}_3$  is very high, e.g. the carrier density of  $\text{La}_{0.5}\text{Sr}_{0.5}\text{TiO}_3$  is about  $8 \times 10^{21}/\text{cm}^3$  [11]. Based on the existing theoretical models of DMS [9], such high carrier density and the associated non-localized nature of the carriers makes it an interesting system to explore from the standpoint of carrier induced ferromagnetism. We note as an aside that  $\text{La}_{1-x}\text{Sr}_x\text{TiO}_3$  is considered to be a prototypical strongly correlated system where the standard band theory picture does not apply.

It has been shown that although single phase  $\text{La}_{1-x}\text{Sr}_x\text{TiO}_3$  ( $x=0.5$ ) can not be easily realized in a sintered bulk compound, a single metallic phase state can be stabilized in epitaxial thin-film form by pulsed-laser deposition [15]. In our work, thin films of  $\text{La}_{1-x}\text{Sr}_x\text{Ti}_{1-y}\text{Co}_y\text{O}_{3-\delta}$  ( $x= 0.5, 0.3, y=0, 0.01, 0.015, 0.07$ ) were grown on  $\text{SrTiO}_3$  (001) and  $\text{LaAlO}_3$  (001) substrates at 700 °C by pulsed laser deposition with KrF excimer laser pulses (248 nm). The targets were prepared by a standard solid state reaction method. The energy density and repetition rate were  $1.8 \text{ J/cm}^2$  and 10 Hz, respectively. Depositions were performed at different oxygen pressures over the range from  $3 \times 10^{-6}$  Torr to  $10^{-2}$  Torr. After deposition, the films were cooled to room temperature at 30 °C/min at the same pressure. The films were characterized by various techniques such as x-ray diffraction, four probe electrical resistivity measurements, SQUID and vibrating sample magnetometries (VSM), Rutherford backscattering (RBS) and ion channeling, field emission scanning transmission electron microscopy (STEM, 0.14 nm probe size) for Z-contrast imaging, and electron energy loss spectroscopy (EELS).

Fig.1(a) shows the x-ray diffraction pattern of  $\text{La}_{0.5}\text{Sr}_{0.5}\text{Ti}_{1-y}\text{Co}_y\text{O}_{3-\delta}$  with  $y = 0.015$ , indicating a single phase perovskite structure with (00l) orientation. Similar data were also obtained for films with other concentrations. The rocking curve full width at half maximum (FWHM) is  $\sim 0.3^\circ$ , establishing the high orientational quality of the films. In Fig. 1(b) we compare the x-ray diffraction patterns (200 planes) for  $\text{La}_{0.5}\text{Sr}_{0.5}\text{Ti}_{1-y}\text{Co}_y\text{O}_{3-\delta}$  films with  $y = 0.0$  (undoped) and  $y = 0.015$ . A small shift of the film (002) peak to lower  $2\theta$  value (corresponding to expanded  $d_{002}$ ) can be clearly noted; while the reference (002) LAO substrate peak for the two cases overlaps exactly. This indicates incorporation of cobalt atoms into the matrix. Fig. 1 (c) shows the magnetization (M) for the  $\text{La}_{0.5}\text{Sr}_{0.5}\text{Ti}_{0.985}\text{Co}_{0.015}\text{O}_{3-\delta}$  grown at an oxygen pressure of  $10^{-4}$  Torr measured by SQUID (5-300K) and VSM ( $>300$  K). It is clear that the film exhibits high temperature ferromagnetism with a Curie temperature close to 450K. Indeed, the inset shows the hysteresis recorded at 423 K, showing a well defined loop with a coercivity of  $\sim 150$  Oe. Another inset in Fig. 1(c) shows the STEM cross-section image of  $\text{La}_{0.5}\text{Sr}_{0.5}\text{Ti}_{1-y}\text{Co}_y\text{O}_{3-\delta}$  with  $y = 0.015$  which confirms the high crystalline quality of the film. Similar STEM image quality was also seen for all other samples. However, in samples with  $y=0.07$  EELS data showed inhomogeneity in cobalt concentration with suggestion of dopant clustering over 1-2 nm size scale. The results discussed below are therefore limited to films with low cobalt concentrations of  $y=0.01$  and  $0.015$ , for which no such inhomogeneity was detected.

Figs. 2(a,b,c) show the temperature dependence of resistivity ( $\rho$ ) for three cases of films of  $\text{La}_{0.5}\text{Sr}_{0.5}\text{Ti}_{1-y}\text{Co}_y\text{O}_{3-\delta}$  with  $y=0.015$ , grown at the oxygen pressures of  $10^{-2}$ ,  $10^{-4}$ , and  $3 \times 10^{-6}$  Torr, respectively. In all the studied samples it was ensured that the films

were single phase perovskite. The typical form in all cases is weak metallicity at and below room temperature and semiconducting nature at lower temperature. The temperature at which the metal-semiconductor transition occurs is seen to shift to higher temperature with increased oxygen pressure during growth. Figs. 2(d,e,f) show the dependence of resistivity on  $T^2$  for the cases in Figs. 2(a,b,c) exhibiting good linearity over the region of metallicity. Such  $T^2$  dependence suggests a strong electron-electron interaction in this compound. With Co doping, the resistivity deviates from the  $T^2$  behavior below a certain temperature, and this temperature increases with  $x$  and  $y$ . The doping-induced change in resistivity and its temperature dependence indicate that Co does dope into the structure of the Ti-based perovskite.

Fig. 2(g) shows the 5K and 300K resistivity values, which follow similar growth pressure dependence and span almost three decades on the resistivity scale, allowing an opportunity to examine the dependence of magnetization on resistivity over a wide range. The resistivity decrease with decrease in oxygen growth pressure implies that conduction in films is controlled significantly by oxygen vacancy concentration. Indeed, preliminary Hall data showed that the density of carriers in this system (which are n-type, as discussed by Tokura et al. [11] ) at room temperature in films grown at  $10^{-2}$  and  $10^{-4}$  Torr is  $\sim 4.5 \times 10^{21} / \text{cm}^3$  and  $9.5 \times 10^{21} / \text{cm}^3$ , respectively. It may further be noted from Fig. 2(g) that the out of plane lattice parameter also shows a relaxation by up to 1.5% over the same range of growth pressures, and the direction of change appears consistent with the expected change in the oxygen vacancy concentration. Indeed, the RBS study under oxygen resonance condition (not shown) reveals oxygen deficiency in the films grown at low oxygen pressures. In Figs. 2(h,i) are shown the dependence of  $\ln(\rho)$  on  $(1/T)^{1/4}$  for

films grown at  $10^{-2}$  and  $10^{-4}$  Torr, respectively. The linearity at very low temperature suggests variable range hopping (VRH) of localized carriers in this range.

In Fig. 3 we show the dependence of magnetization on resistivity at 5K for a set of  $\text{La}_{1-x}\text{Sr}_x\text{Ti}_{1-y}\text{Co}_y\text{O}_{3-\delta}$  samples with  $x = 0.5$  ( $y = 0.015$  and  $y=0.010$ ) and  $x=0.3$ ,  $y=0.015$ . The first, third and fifth filled black circles from right to left correspond to the data of Fig. 2 (a), (b) and (c), respectively. A few important observations can be immediately made. First, ferromagnetism with a significant moment is observed only in samples in the intermediate resistivity range of about  $10^2$  to  $10^4 \mu\Omega\text{-cm}$ , the dependence for the  $y = 0.015$  series examined in more details being non-monotonic with an asymmetric bell shaped nature. Second,  $M$  is significantly higher than its value of  $\sim 1.72 \mu_B/\text{Co}$  for pure cobalt metal. Third, the  $M$ - $\rho$  systematics depend on both  $x$  and  $y$  in  $\text{La}_{1-x}\text{Sr}_x\text{Ti}_{1-y}\text{Co}_y\text{O}_{3-\delta}$ . While these data strongly suggest the role of carrier density and dynamics in the occurrence of ferromagnetism, it is difficult to offer a simple physical picture at this stage due to the coexisting contributions of cobalt ions and oxygen defects to the transport. In particular, the large value of the magnetic moment per cobalt and its dependence on growth pressure may imply presence and evolution of a high-spin and low spin admixture of  $\text{Co(II)}$  and  $\text{Co(III)}$  ions. Such conditions are known to occur for octahedrally coordinated cobalt as in perovskite matrices [16,17]. Other possibilities such as a partial transferred moment on Ti may also have to be addressed by further experiments. In the inset of Fig. 3 are shown representative magnetoresistance data for the  $\text{La}_{0.5}\text{Sr}_{0.5}\text{Ti}_{1-y}\text{Co}_y\text{O}_{3-\delta}$  sample with  $y = 0.015$  grown at  $10^{-4}$  Torr. Significant negative magnetoresistance ( $\text{MR} = (\rho_H - \rho_0)/\rho_0 \times 100 \%$ ) is seen only at very low temperatures when the resistivity exhibits VRH as discussed earlier (Fig. 2(i)). The MR typically

shows an initial drop with increasing magnetic field, followed by an increase above a certain intermediate field value. Such interesting behavior has also been reported in other VRH systems, and is attributed to an interplay of quantum interference effects at low fields and orbital shrinkage at high fields [18,19].

Finally, in Fig. 4 we show the magnetic and optical properties of the relatively resistive  $\text{La}_{0.5}\text{Sr}_{0.5}\text{Ti}_{1-y}\text{Co}_y\text{O}_{3-\delta}$  sample with  $y = 0.015$  grown at  $10^{-2}$  Torr. The temperature dependence of  $M$  (inset) shows a  $T_C$  close to  $\sim 550\text{K}$ , about  $100\text{K}$  higher than that for the relatively conducting film grown at  $10^{-4}$  Torr (Fig. 1(c)). Notably, the decrease of magnetization to zero value is gradual for the resistive film (Fig. 4, inset) as compared to that for the conducting film (Fig. 1(c)). In the case of more resistive samples a mechanism of magnetic polaron percolation has been suggested for DMS systems [20]. In such a scenario a more gradual build up of magnetization with lowering of temperature could be expected. Other possibilities such as development of nanoscale inhomogeneities under these relatively more oxidizing conditions could not be completely ruled out. It may further be noted from the optical transmission data and the picture in the inset that film grown under such high pressure qualifies to be a transparent diluted magnetic system.

In conclusion, ferromagnetism is observed at and above room temperature in epitaxial  $\text{La}_{1-x}\text{Sr}_x\text{Ti}_{1-y}\text{Co}_y\text{O}_{3-\delta}$  perovskite films deposited over a range of oxygen pressures. It is shown that ferromagnetism is realized in both opaque metallic as well as transparent semiconducting films. The dependence of the magnetic and transport properties on  $x$ ,  $y$  and  $\delta$  suggests that the ferromagnetism is carrier-induced.



This work was supported by NSF under the MRSEC grant DMR-00-80008, by DARPA (T.V, S.B.O) by US-ONR (S.D.S) and DARPA (S.D.S), and New Jersey Commission on Higher Education (S.L.). Two of the authors (J.P.B and N.D.B) would like to acknowledge DOE funding under grant DE-FG02-96ER45610 and NSF support for the purchase of the JEOL microscope under grant DMR-9601792.

¶ On leave from Tsinghua University, China.

\* Also at the Department of Materials Science and Nuclear Engineering,  
[ogale@squid.umd.edu](mailto:ogale@squid.umd.edu)

§ On leave from Indian Institute of Technology, Kanpur, India.

## References

1. G. A. Prinz, Science **282**, 1660 (1998); H. Ohno, Science **281**, 951 (1998); S. A. Wolf, et al. Science, **294**, 1488 (2001), Y. D. Park et al., Science **295**, 651 (2002).
2. S. Das Sarma, American Scientist, **89**, 516 (2001).
3. H. Ohno, A. Shen, F. Matsukura, A. Oiwa, A. Endo, S. Katsumoto, and Y. Iye, Appl. Phys. Lett. **69**, 363 (1996).
4. T. Fukumura, Z. Jin, A. Ohtomo, H. Koinuma, and M. Kawasaki, Appl. Phys. Lett. **75**, 3366 (1999).
5. K. Ando, H. Saito, Z. Jin, T. Fukumura, M. Kawasaki, Y. Matsumoto, and H. Koinuma, J. Appl. Phys. **89**, 7284 (2001).
6. K. Ueda, H. Tabata, and T. Kawai, Appl. Phys. Lett. **79**, 988 (2001).
7. Y. Matsumoto, M. Murakami, T. Shono, T. Hasegawa, T. Fukumura, M. Kawasaki, P. Ahmet, T. Chikyow, S. Koshihara, and H. Koinuma, Science **291**, 854 (2001).
8. Y. Matsumoto, R. Takahashi, M. Murakami, T. Koida, X. J. Fan, T. Hasegawa, T. Fukumura, M. Kawasaki, S. Koshihara, and H. Koinuma, Jpn. J. Appl. Phys. **40**, L1204 (2001).

9. T. Dietl, H. Ohno, F. Matsukura, J. Cibert, and D. Ferrand, *Science* **287**, 1019 (2000), A. Chattopadhyay, S. Das Sarma and A. J. Millis, *Phys. Rev. Lett.* **87**, 227202 (2001), *ibid* *Phys. Rev.* **B64**, 012416 (2001).
10. S. B. Ogale, S. Das Sarma, A. J. Millis and T. Venkatesan (unpublished).
11. Y. Tokura, Y. Taguchi, Y. Okada, Y. Fujishima, T. Arima, K. Kumagai, and Y. Iye, *Phys. Rev. Lett.* **70**, 2126 (1993).
12. D. A. Crandles , T. Timusk, and J. E. Greedan, *Phys. Rev.* **B44**, 13250 (1991): D. A. Crandles , T. Timusk, J. D. Garrett, and J. E. Greedan, *Physica* **201C**, 407 (1992).
13. Y. Maeno, S. Awaji, H. Matsumoto, and T. Fujita, *Physica* **165-166B**, 1185 (1990).
14. Y. Fujishima, Y. Tokura, T. Arima, and S. Uchida, *Phys. Rev.* **B46**, 11167 (1992).
15. W. Wu, F. Lu, K. H. Wong, Geoffrey, C. L. Choy, and Y. Zhang, *J. Appl. Phys.* **88**, 700 (2000).
16. Y. Morimoto, K. Higashi, K. Matsuda, and A. Nakamura, *Phys. Rev.* **B55**, R14725 (1997).
17. V. Primo-Martin and M. Jansen, *J. Solid State Chem.* **157**, 76 (2001).
18. M. E. Raikh, J. Czingon, Q. Ye, F. Koch, W. Schoepe, and K. Ploog, *Phys. Rev.* **B45**, 6015 (1992)
19. J. R. Friedmann, Y. Zhang, P. Dai, and M. P. Sarachik, *Phys. Rev.* **B53**, 9528 (1996).
20. A. Kaminski and S. Das Sarma, *Phys. Rev. Lett.* **88**, 247202 (2002).

Figure Captions :

Fig. 1: (a) A typical x-ray diffraction (XRD) pattern of the  $\text{La}_{0.5}\text{Sr}_{0.5}\text{Ti}_{0.985}\text{Co}_{0.015}\text{O}_3$  film, (b) Comparison of XRD patterns for  $\text{La}_{0.5}\text{Sr}_{0.5}\text{Ti}_{1-y}\text{Co}_y\text{O}_3$  films with  $y = 0.0$  (undoped) and  $y = 0.015$ , (c) M-T curve for the  $\text{La}_{0.5}\text{Sr}_{0.5}\text{Ti}_{0.985}\text{Co}_{0.015}\text{O}_3$  film. The inset shows hysteresis loop at 423 K. Second inset shows the STEM image.

Fig. 2: Temperature dependence of resistivity for the  $\text{La}_{0.5}\text{Sr}_{0.5}\text{Ti}_{0.985}\text{Co}_{0.015}\text{O}_3$  films grown at (a)  $10^{-2}$ , (b)  $10^{-4}$ , and (c)  $3 \times 10^{-6}$  Torr. The resistivity data shown in (a), (b), and (c) is plotted as a function of  $T^2$  in (d), (e), and (f), respectively. The 300 and 5 K resistivity and the (200) lattice parameter measured at 300 K for the films grown at different oxygen pressures are shown in (g). The  $\ln(\rho)$  for the films grown at  $10^{-2}$  and  $10^{-4}$  Torr is plotted as a function of  $(1/T)^{1/4}$  in (h) and (i), respectively.

Fig. 3: The saturation magnetization at 5 K plotted as a function of 5 K resistivity for the  $\text{La}_{1-y}\text{Sr}_y\text{Ti}_{1-x}\text{Co}_x\text{O}_3$  films. The lines drawn are guides to the eye. The first, third and fifth filled black circles from right to left correspond to the data of Fig. 2 (a), (b) and (c), respectively. The inset shows the magnetoresistance data at different temperatures for the  $\text{La}_{0.5}\text{Sr}_{0.5}\text{Ti}_{0.985}\text{Co}_{0.015}\text{O}_3$  film.

Fig. 4: (a) Optical transmission spectrum for the  $\text{La}_{0.5}\text{Sr}_{0.5}\text{Ti}_{0.985}\text{Co}_{0.015}\text{O}_3$  film grown at  $10^{-2}$  Torr. The transparency in the visible range is clearly demonstrated by the photograph at the upper left corner. The high temperature M-T curve for this film is shown in inset.

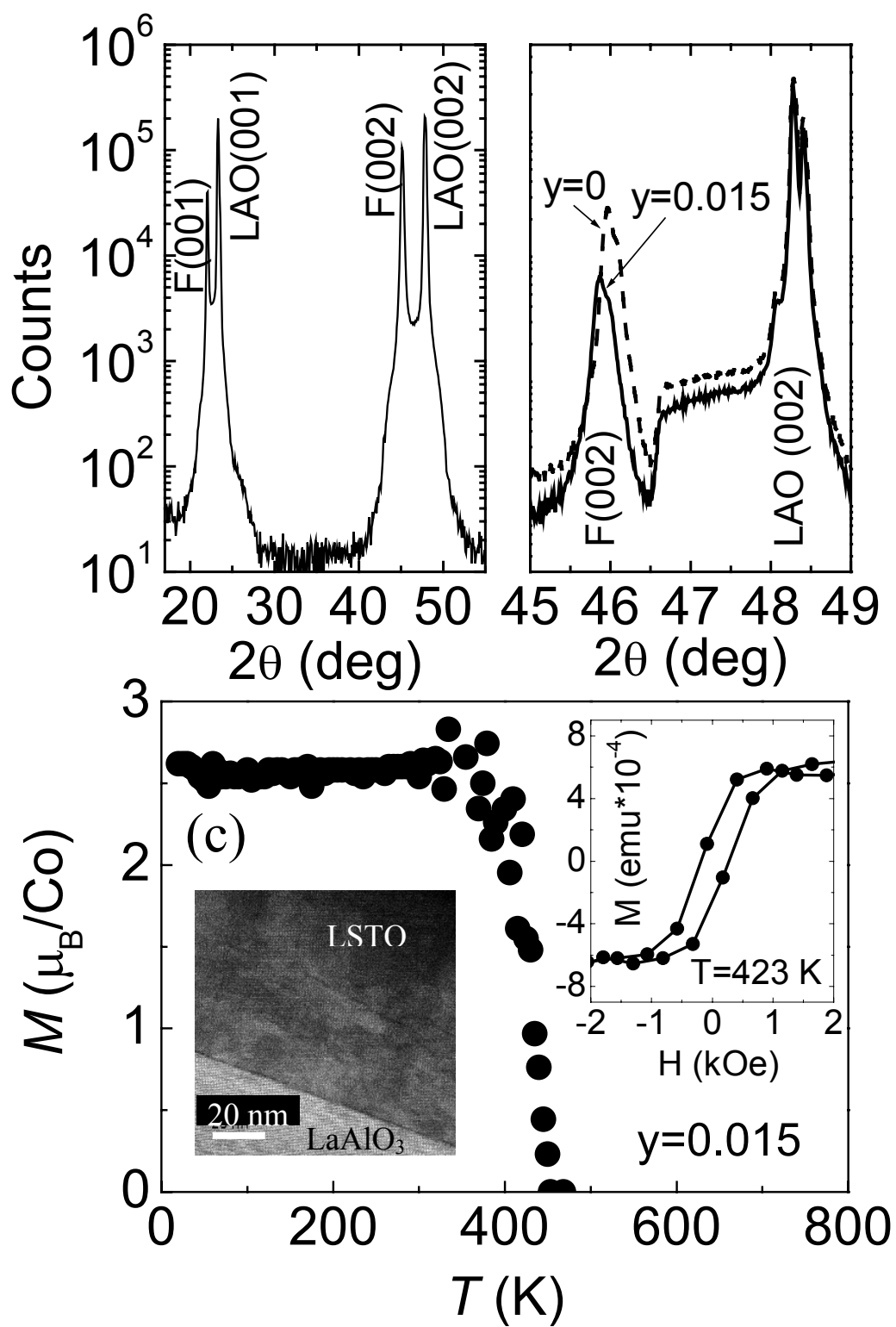


Figure 1: Zhao et al.

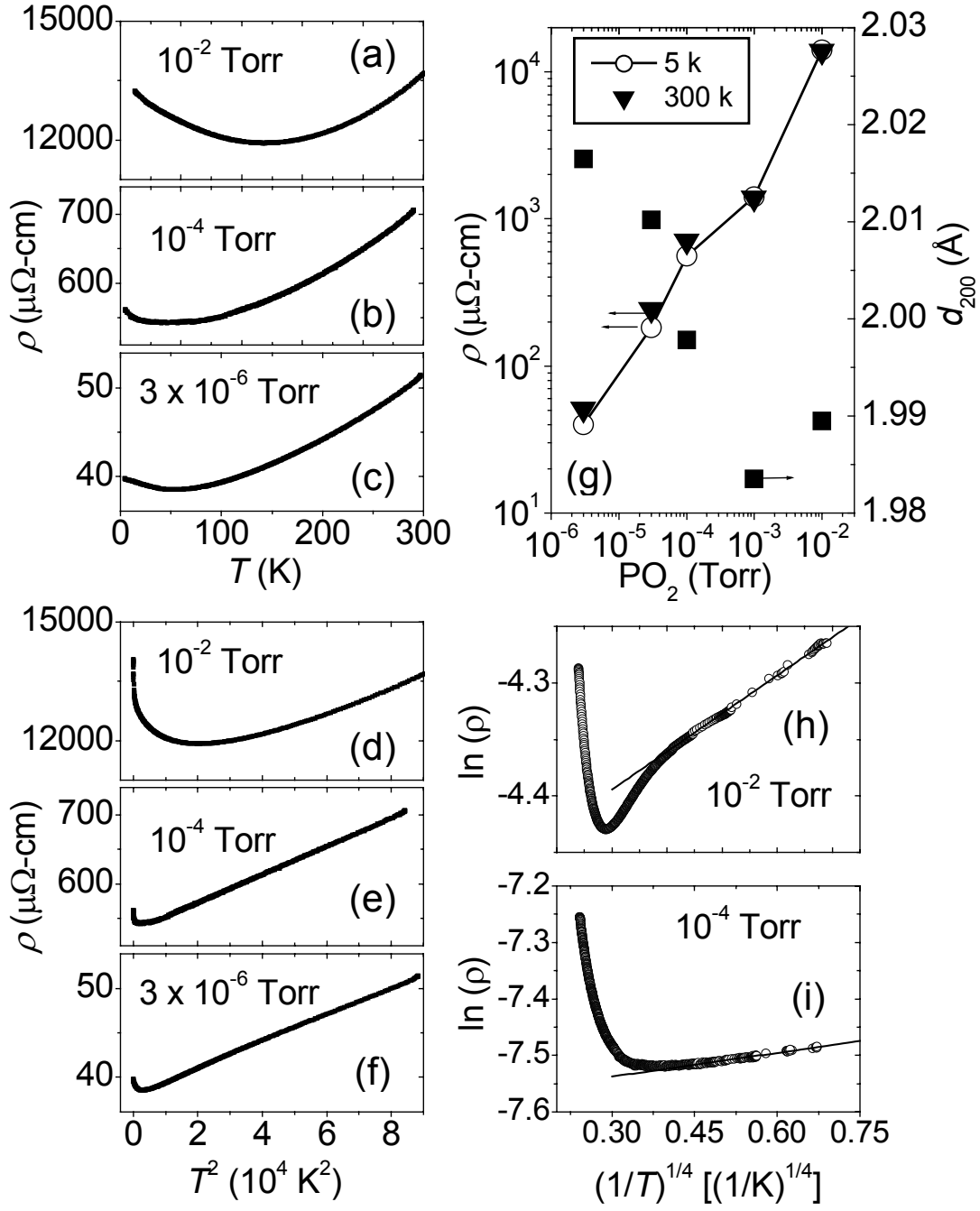


Figure 2: Zhao et al.

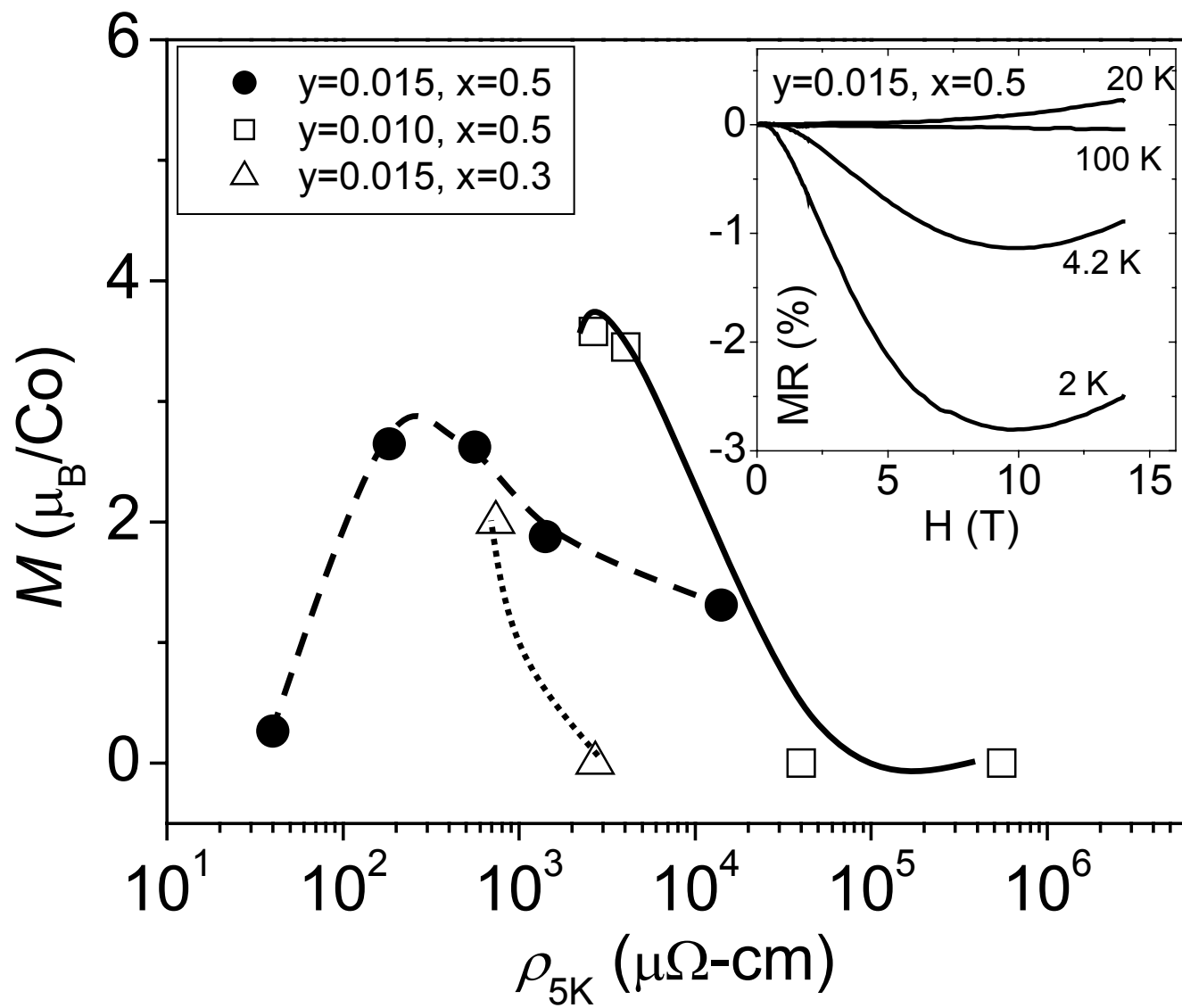


Figure 3: Zhao et al.

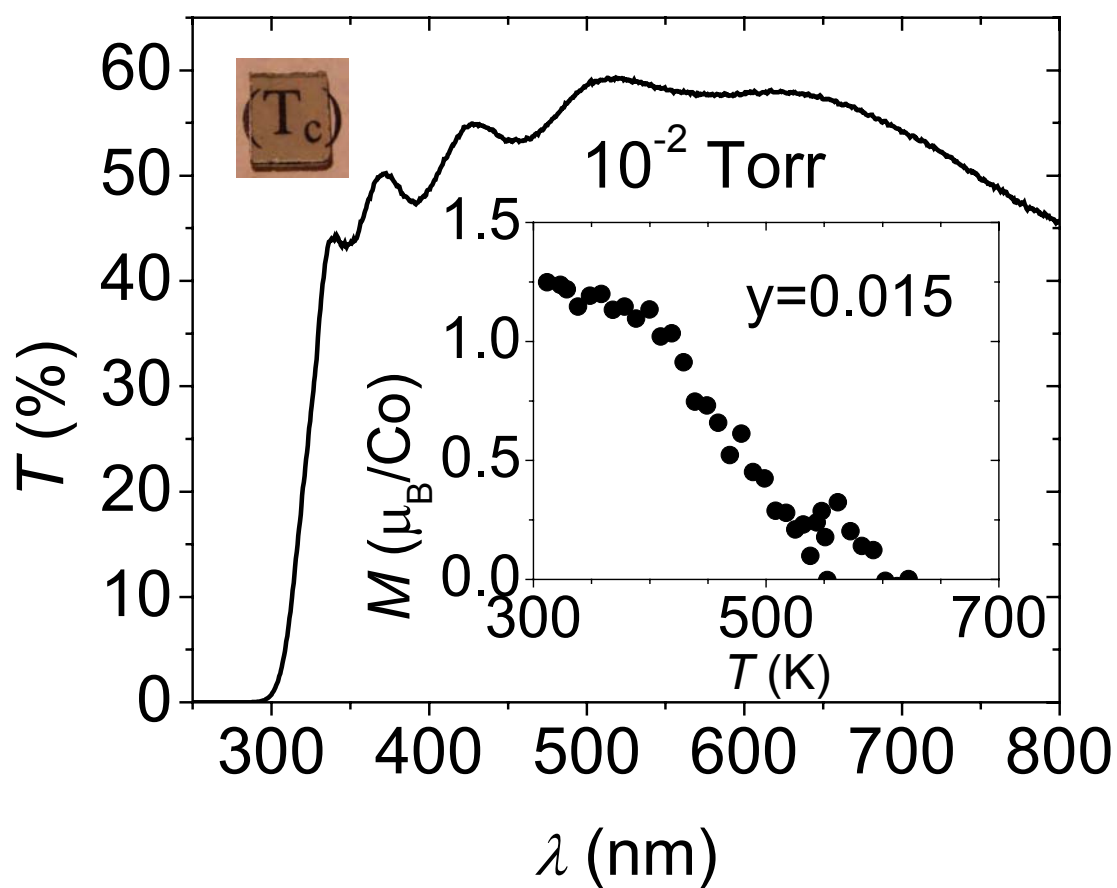


Figure 4: Zhao et al.